Fast and Selective Sugar Conversion to Alkyl Lactate and Lactic Acid with Bifunctional Carbon–Silica Catalysts

ARTICLE *in* JOURNAL OF THE AMERICAN CHEMICAL SOCIETY · MAY 2012

Impact Factor: 12.11 · DOI: 10.1021/ja301678w · Source: PubMed

JACS
JOURNAL OF THE AMERICAN CHEMICAL SOCIETY

Article

pubs.acs.org/JACS

Fast and Selective Sugar Conversion to Alkyl Lactate and Lactic Acid with Bifunctional Carbon–Silica Catalysts

Filip de Clippel,[†,∥] Michiel Dusselier,[†,∥] Ruben Van Rompaey,[†] Pieter Vanelderen,[†] Jan Dijkmans,[†] Ekaterina Makshina,[†] Lars Giebeler,[‡] Steffen Oswald,[‡] Gino V. Baron,[§] Joeri F. M. Denayer,[§] Paolo P. Pescarmona,[†] Pierre A. Jacobs,[†] and Bert F. Sels*[,†]

[†]Center for Surface Chemistry and Catalysis, Katholieke Universiteit Leuven, Kasteelpark Arenberg 23, 3001 Heverlee, Belgium

[‡]Institute for Complex Materials, Leibniz-Institute for Solid State and Materials Research, Helmholtzstraβe 20, D-01069 Dresden, Germany

[§]Department of Chemical Engineering, Vrije Universiteit Brussel, Pleinlaan 2, 1050 Elsene, Belgium

Supporting Information

ABSTRACT: A novel catalyst design for the conversion of mono- and disaccharides to lactic acid and its alkyl esters was developed. The design uses a mesoporous silica, here represented by MCM-41, which is filled with a polyaromatic to graphite-like carbon network. The particular structure of the carbon-silica composite allows the accommodation of a broad variety of catalytically active functions, useful to attain cascade reactions, in a readily tunable pore texture. The significance of a joint action of Lewis and weak Brønsted acid sites was studied here to realize fast and selective sugar conversion. Lewis acidity is provided by grafting the silica component with Sn(IV), while weak Brønsted acidity originates from oxygen-containing functional groups in the carbon part. The weak Brønsted acid content was varied by changing the amount of carbon loading, the pyrolysis temperature, and the post-treatment procedure. As both catalytic functions can be tuned independently, their individual role and optimal balance can be searched for. It was thus demonstrated for the first time that the presence of weak Brønsted acid sites is crucial in accelerating the rate-determining (dehydration) reaction, that is, the first step in the reaction network from triose to lactate. Composite catalysts with well-balanced Lewis/Brønsted acidity are able to convert the trioses, glyceraldehyde and dihydroxyacetone, quantitatively into ethyl lactate in ethanol with an order of magnitude higher reaction rate when compared to the Sn grafted MCM-41 reference catalyst. Interestingly, the ability to tailor the pore architecture further allows the synthesis of a variety of amphiphilic alkyl lactates from trioses and long chain alcohols in moderate to high yields. Finally, direct lactate formation from hexoses, glucose and fructose, and disaccharides composed thereof, sucrose, was also attempted. For instance, conversion of sucrose with the bifunctional composite catalyst yields 45% methyl lactate in methanol at slightly elevated reaction temperature. The hybrid catalyst proved to be recyclable in various successive runs when used in alcohol solvent.

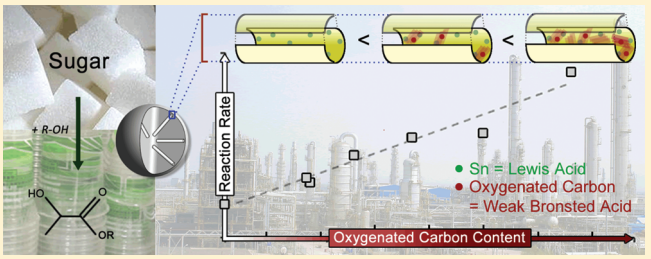

INTRODUCTION

There has been a growing interest in deriving chemicals from biomass resources.[1] Among the products of interest, lactic acid is considered a key platform molecule in such a biobased economy. Lactic acid is generally obtained by fermentation of common sugars, and it is often used as such in detergents, cosmetics, and as a food additive. Lactic acid is also commonly used as antibacterial agent in disinfecting products.[2,3] Recent scientific interest in lactic acid has intensified due to its use in biodegradable plastics. The worldwide production of synthetic plastics, annually increasing with 5% during the last 20 years, totaled about 265 million tons in 2010.[4] Most of these plastics are oil-derived and as such neither sustainable nor environmentally friendly.[5] Research efforts nowadays are focused in finding alternative polymers, which are biodegradable, while preserving the stability, durability, and functionality of traditional plastics. Furthermore, as the oil price and, therefore, the demand for sustainable feedstocks are increasing annually, biodegradable biomass-derived plastics will be preferred over biodegradable synthetic plastics.[6] Polylactic acid or polylactide (PLA), as discovered by DuPont in 1932, is one of the main candidates for future biopolymers. PLA is obtained by ring-opening polymerization of lactide, the cyclic dimer of lactic acid. The mechanism of this reaction has been studied extensively for the past two decades.[7] In 2010, the bioplastics production capacity totaled 0.72 million tons, which comprised only 0.3% of the total plastic production.[8] However, global bioplastic production is increasing annually about 40%, emphasizing the importance of PLA and lactic acid research.[9,10]

Received: February 20, 2012
Published: May 2, 2012

   dx.doi.org/10.1021/ja301678w | J. Am. Chem. Soc. 2012, 134, 10089–10101

Besides being used to prepare polymers, lactic acid can also serve as a building block for other interesting chemicals. Catalytic dehydration and hydrogenation, for instance, leads to acrylic acid and propylene glycol, respectively.[11] Lactate esters also represent a vast market of applications. Short chain esters such as ethyl lactate are considered green solvents and are an important raw material for the skin care industry.[3,12] Long chain alkyl lactates such as dodecyl lactate are frequent in cosmetics and healthcare formulations as moisturizers and solvents.[13]

Lactic acid is mainly produced by fermentation of glucose obtained from starch or cellulose-containing material. Such carbohydrates are abundant in agricultural resources such as corn, wood, wheat, and rice.[6,14] Cellulose, together with lignin and hemicellulose, is considered to be a key substrate in the future chemical industry as it does not interfere with food supply.[1,15] Because of acid inhibition, continuous buffering during the fermentation is essential, but results in the formation of 1 ton gypsum per ton of lactic acid.[3,6,16] Hence, extensive purification and separation hamper large-scale operation. Alkyl lactate esters are usually produced by esterification of lactic acid with the corresponding alcohols.

New methods to synthesize lactic acid and alkyl lactates using homogeneous and heterogeneous Lewis acid catalysts have been proposed recently from trioses, glyceraldehyde (GLY) and dihydroxyacetone (DHA).[17−21] Both trioses can be obtained catalytically or biochemically from formaldehyde or bioderived glycerol.[22,23] The direct conversion of glycerol into lactic acid has also been reported.[24] Recent research describes the direct enzyme-free conversion of hexoses such as glucose, fructose, and sucrose into alkyl lactate (Figure 1).[21,25] The conversion involves initial isomerization of aldose into ketose, followed by retro-aldol to the corresponding trioses, GLY and DHA.

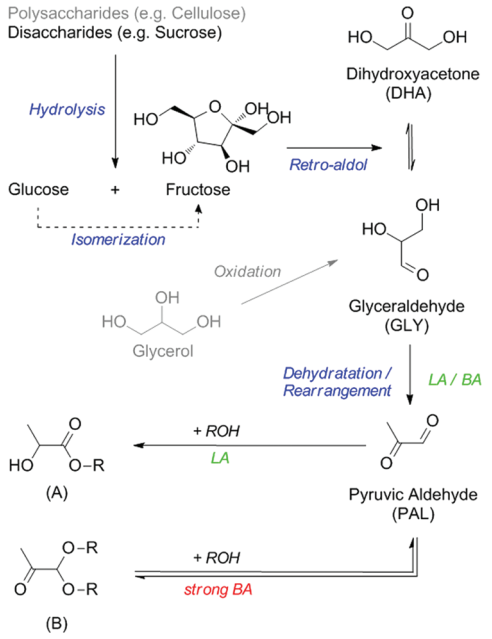

Figure 1. Proposed reaction scheme for converting monosaccharides such as trioses and aldo- and ketohexoses like fructose into lactic acid in aqueous medium (R = H) or into alkyl lactates (A) in alcoholic solvents (R = alkyl). The side-reaction leading to the formation of pyruvic aldehyde dialkyl acetal (B) is undesired; LA = Lewis acid and BA = Brønsted acid.

Various mechanisms have been proposed to explain the conversion of biomass-derived dihydroxyacetone (DHA) and glyceraldehyde (GLY) to alkyl lactates.[17,18] It is generally accepted that three main reaction steps occur in the reaction network (Figure 1). First, GLY in equilibrium with DHA[26] is converted by dehydration and rearrangement into pyruvic aldehyde (PAL), which in our opinion is catalyzed both by Lewis acid (LA) and by Brønsted acid (BA) groups.[19b,20] Weak Brønsted acids such as acetic acid have been demonstrated to sufficiently catalyze the PAL formation.[19b] PAL is further converted under action of a Lewis acid into the desired alkyl lactates or lactic acid in alcoholic solvents and water, respectively. The mechanism of this last step is under debate. A formal intramolecular Cannizzaro and a redox mechanism involving Meerwein−Ponndorf−Verley reduction and Oppenauer oxidation have been suggested.[19] The presence of strong Brønsted acid groups should be avoided because they catalyze the formation of the undesirable acetal byproduct in a parallel reaction path (Figure 1).

Efficient sugar conversion requires a good balance between the reaction kinetics in the overall reaction network. This requirement thus underlines the search toward catalyst designs focusing on multifunctionality. We kindly refer here to some recent examples wherein such multifunctional catalysis is key.[27] Formation of PAL from GLY (and DHA) is likely rate determining because PAL is only present in trace amounts in the catalytic solution. This observation agrees with the higher activation energy of PAL formation (93 ± 3 kJ mol^{-1}) when compared to that of the subsequent lactate formation (58 ± 14 kJ mol^{-1}).[18d] Improvement in conversion rate (per Lewis acid site) and product selectivity is thus to be expected after balancing the two acid types; that is, Lewis acid sites require sufficient weak Brønsted acid sites. This hypothesis will be the key subject in this catalytic study.

So far, Lewis acid zeotypes, for example, Sn-Beta and Lewis/Brønsted acid mesoporous catalysts like Al-rich USY and Al, Ti, Ga, or Sn doped silica, have been tested.[18−20] Their mutual dependency of Lewis and Brønsted acid content complicates the independent control of the amount and strength of each functional group, and thus the search for their optimal balance. Herein, hybrid materials may offer new possibilities toward flexible, multifunctional catalysis.[28] We here present the design of a bifunctional (Lewis and weak Brønsted) catalyst based on our previously reported carbon-silica composite material (CSM).[29] This CSM is constructed of two components, silica such as MCM-41, which is filled with a porous (polyaromatic hydro)carbon network. Such composite material has been used earlier as precursor of mesoporous carbon,[30] as molecular sieve,[29,31] or in monofunctional catalysis,[32] but its potential in multifunctional catalysis was not yet explored. This contribution addresses the use of these CSMs as catalyst in the conversion of sugars into lactic acid in aqueous solution and into alkyl lactate in alcoholic media, according to the reaction scheme in Figure 1. Modification of the organic and inorganic constituents of the CSM with catalytic sites creates a multifunctional catalyst, which will prove beneficial in the sugar conversion. As each component bears one acid type, the population of Brønsted and Lewis acid sites can be tuned independently. Briefly, the silica component is grafted with Lewis acid Sn(IV), while the intraporous carbon is decorated with various surface functional groups exhibiting mild Brønsted acidity. Optionally, the content of the latter groups is easily enhanced by an additional thermal treatment in oxygen. Both

the amount of carbon and the oxidation procedure affect the sugar conversion rate and the product selectivity. Composite catalysts, optimally engineered as described in this article, are very active and selective for the title sugar conversion.

EXPERIMENTAL SECTION

Catalyst Synthesis. Micelle-templated spherical Si-MCM-41 silica particles have been synthesized according to a modified Stöber method as described by Grün et al.[33] Cetyl trimethylammonium bromide (CTAB, ACROS) was selected as cationic surfactant and dissolved in Millipore water. Next, ethanol (VWR) was added to enhance dissolution of the surfactant followed by a mineralizing agent, ammonium hydroxide, to adjust the pH value at 11. After 15 min, TEOS (Fluka) was added to obtain a final gel composition of $1Si(OEt)_4$:0.3CTAB:$11NH_3$:$144H_2O$:58EtOH. The gel was stirred for 2 h at room temperature. The obtained solid was thoroughly washed with Millipore water until a neutral pH was obtained, dried at 343 K overnight, and finally calcined in air for 8 h in a muffle furnace at 823 K (1 K min^{-1}). Lewis acid sites were introduced by liquid-phase grafting. Dried Si-MCM-41 powder was refluxed in N_2 atmosphere with a 0.26 M solution of anhydrous Sn(IV) chloride (99%, Aldrich) in isopropanol (IPA) (100 mL g^{-1}; 99.5+%, ACROS) for 12 h. Next, the grafted silica was washed four times with IPA (500 mL g^{-1}) and dried at 333 K overnight. Finally, the Sn oxide modified silica, further denoted as Sn-Si-MCM-41, was obtained by calcination in air at 823 K for 6 h (1 K min^{-1}).[34] Sn-Si-MCM-41 was used as such as the reference catalyst to distinguish the effect of the presence of oxidized carbon, and as template to obtain the CSM catalysts with varying carbon content.

CSMs were prepared by introducing a carbon precursor solution into the pores of Sn-Si-MCM-41 by incipient wetness impregnation. This solution consists of furfuryl alcohol (FA), which acts as carbon precursor, and mesitylene, a diluting agent for controlling the amount of deposited carbon. More experimental and physicochemical details are reported elsewhere.[29] Key in the procedure is the volume match between the impregnation solution and the pores. The sample was then heated to 423 K (5 K min^{-1}) in a He stream (50 mL min^{-1}) for 6 h to initiate in situ polymerization of FA and subsequent pyrolysis at various temperatures (673 K until 1173 K) for 4 h. Optional postsynthesis oxidation was performed by transferring 0.2 g of CSM powder into a glass tube with a diameter of 0.8 cm. Subsequently, the sample was heated (5 K min^{-1}) for 8 h at various temperatures (473−673 K) under oxygen flow at a rate of 30 mL min^{-1}.

In the following sections, CSM catalysts will be denoted as Sn-Si-CSM-X-Y/Z in which X, Y, and Z represent the pyrolysis temperature (in K), the carbon fraction (in wt %), and the postsynthesis oxidation method, respectively.

Characterization. Successful synthesis of the mesoporous silica template and its Sn analogue was confirmed with X-ray powder diffraction (XRD) and N_2 sorption. Pore ordering and structure were analyzed by XRD with a STOE STADI P diffractometer equipped with a Ge(111)-Johann-type monochromator and a 140°-position sensitive image plate detector at room temperature. All samples were measured in Debye−Scherrer geometry using Cu $K_{\alpha 1}$ radiation. Porosity and texture were determined by nitrogen adsorption using the Tristar 3000 (Micromeritics Instr.) equipment. Sorption experiments were performed at liquid nitrogen temperature, and equilibration was allowed for each experimental data point. All samples were degassed under nitrogen flow at 673 K overnight prior to the measurement. Pore size distributions were obtained from nitrogen adsorption isotherms as recorded on an Autosorb-1 instrument (Quantachrome, U.S.) at 77 K. The samples were evacuated at 523 K under vacuum for 12 h, and the NLDFT model was applied on the adsorption branch (cylindrical pore model).

Analysis of Lewis acidity due to the presence of Sn was carried out by pyridine probe FT-IR spectroscopy. A self-supporting Sn-Si-MCM-41 wafer was dried in vacuo at 673 K and saturated with about 25 mbar of pyridine vapor at room temperature for 10 min. Next, the sample was put under vacuum and heated at 323 K to remove physisorbed pyridine. Finally, Brønsted and Lewis characteristic pyridine peaks of Sn-Si-MCM-41 were examined at various temperatures. The evacuated sample containing chemisorbed pyridine was subjected to a temperature-programmed desorption at 323, 373, 423, and 473 K for 30 min, respectively, with a heating rate of 4 K min^{-1}, and the IR spectra were recorded in situ at these temperatures.

For ICP-OES analysis, a Perkin-Elmer Optima 3300 DV was used to quantify the amount of Sn (189.9 nm) grafted onto the silica and to evaluate Sn leaching during the reaction. Solid silica was dissolved in 1 M NaOH (50 mL g^{-1}) solution prior to analysis. A blank solution was prepared to avoid matrix interferences. The detection limit of Sn was found to be ~3 $\mu g\ L^{-1}$.

The coordination and speciation of tin oxide species were examined by UV−vis diffuse reflectance spectroscopy (DRS). Spectra were recorded on an Agilent Carry 5000 spectrophotometer using $BaSO_4$ as reference. Sn-Si-MCM-41 was measured before and after drying overnight at 473 K in helium flow.

The carbon content of CSMs was determined by thermal gravimetric analysis (TGA). Combustion was performed by bringing the samples into a temperature-programmed oven under an oxidative atmosphere (O_2:N_2 = 9), using a TGA Q500 (TA Instruments) equipped with an automatic sampler, up to 1073 K (10 K min^{-1}). The amount of carbon was calculated from the mass loss taking into account weight loss due to water desorption below 423 K.

The presence and electronic state of the elements Sn, C, and Si were analyzed by X-ray photoelectron spectroscopy (XPS). The experiments were conducted on a Physical Electronics PHI 5600 CI with monochromatized Al $K_{\alpha 1}$ radiation (1486.7 eV) in an energy range of 0−1000 eV. The spectrometer is equipped with a hemispherical analyzer allowing high sensitivity and high-resolution experiments. Samples were pressed into pellets (3000 kg cm^{-2}) to avoid movement of the powder. The sample chamber is held at a pressure of around 10^{-9} mbar. A charge neutralizer with low energy electrons of ca. 5 eV/2−3 μA was applied. The high-resolution spectra were taken with a pass energy of 29 eV and a step size of 0.1 eV. The binding energy is corrected to Si $2p_{3/2}$ at 103.3 eV (for SiO_2). For the deconvolution procedure, a Shirley background subtraction function was primarily applied. Peak position and half width parameter (FWHM) were kept constant, and only the height was fitted by a pseudo-Voigt function. All deconvolutions were performed within the program package PHI-Multipak.[35]

Oxygen surface groups of CSM samples were further analyzed by temperature-programmed desorption (TPD-MS) experiments carried out in a flow apparatus with helium as carrier gas (10 mL min^{-1}), equipped with a Pfeiffer Omnistar quadrupole mass spectrometer for detection of the evolved gases. Prior to the analysis, all samples were flushed in He for 30 min at 303 K. For each experiment, 80 mg of sample was heated from 303 to 1273 K at 10 K min^{-1} while monitoring the evolution of CO (m/z = 28) and CO_2 (m/z = 44). The setup is calibrated with calcium oxalate monohydrate according to a reported procedure.[36]

Additional analysis of the Brønsted acid strength and content was examined by ^{31}P MAS NMR. Spectra were recorded on a Bruker AMX300 spectrometer (7.0 T). 1046 scans were accumulated with a recycle delay of 60 s; the pulse length was set at 2.0 μs. The samples were packed in 4 mm rotors, and the spinning frequency of the rotor was 6 kHz. A solution of 2 mL of orthophosphoric acid (Normapur analytical reagent, VWR, 85%) in 2 mL of water was used as chemical shift reference. Preparation and handling of the NMR samples were carried out with care in a N_2 glovebox. Samples depicted for adsorption of trimethylphosphine oxide (TMPO) were first evacuated for 2 h at 423 K after which TMPO (0.02 M in THF, ACROS) was added (25 mL g^{-1} sample) and allowed to interact for 20 h. Finally, after evacuation of the solvent at room temperature, the samples were transferred into a 4 mm ZrO_2 rotor.

Catalytic Testing. Catalyst powders (0.1 g) were transferred into a glass vial together with all reagents. In a typical catalytic test with trioses, 0.09 g (0.2 M) of DHA (dimer; ACROS) or GLY (ACROS) was dissolved in 5 mL of alcohol, methanol, ethanol, octanol, decanol, dodecanol, and tetradecanol, or Millipore water. 1,4-Dioxane

(ACROS; 0.05 g) was chosen as internal standard when working in alcoholic media. The glass vials were closed by a septum and placed into a multi vial heating block at 363 or 383 K. The mixture was allowed to react for 6 h under continuous magnetic stirring (300 rpm). For the kinetic experiments, samples were taken at regular time intervals. Alkyl lactates were analyzed by gas chromatography on a 30 m Agilent HP-5 column. A selection of chromatograms is illustrated in the Supporting Information. As only lactate, PAL, and acetal products were detected, the conversion was determined by the ratio of their combined amount of moles to the initial amount of moles of trioses. Product yields were calculated with the internal standard taking into account the respective sensitivity factors. Mass balance calculations based on the respective yields of the three products reveal only minor formation of other byproducts. Likewise, the selectivity of alkyl lactate was determined by the molar ratio of alkyl lactate to the total molar amount of alkyl lactate, PAL, and their acetals. Alkyl lactate yields of the higher alcohols were determined accordingly, although quantification of the products was done using relative response factors as obtained by ECN-based calculations.[37] For the analysis of reactions performed in water, an Aminex H87 column with 0.005 M H_2SO_4 as eluent (0.5 mL min^{-1}) was used. A representative chromatogram is shown in the Supporting Information. Yields and conversion were calculated from measured reference lines using commercial samples of the various compounds.

Recycling tests were performed to examine the stability of the CSM catalysts. The supernatant was removed after reaction and examined by GC analysis. The residual catalyst powder was then washed by five cycles of successive addition of 7 mL of solvent, centrifugation, and removal of the liquid. Finally, the powder was dried overnight in the oven at 343 K, and fresh reaction components were added to start the next reaction cycle. Residual activity in the supernatants was also verified.

Conversions of mono- or disaccharides of various hexoses and erythrose were performed in steel batch reactors. 0.225 g of saccharide, 0.150 g of catalyst, and 8 mL of methanol were added and magnetically stirred. Naphthalene was used as internal standard (0.125 g). After four cycles of purging the reactor with N_2, the pressure was set to 20 bar with N_2 and the autoclave was positioned in a copper heating block. The temperature was monitored by a thermocouple inside the vessel. Identification of the reaction products was obtained by GC–MS analysis, HPLC and GC based on retention times of commercial reference chemicals. Product yields were determined as described above for DHA reactions in alcohol using the appropriate sensitivity factors. Additionally, nonvolatile carbohydrates were identified and quantified by HPLC (Agilent 1200 Series) on a Varian Metacarb 67C column (300 × 6.5 mm) using measured reference lines as obtained from solutions containing various amounts of the commercial chemicals. Sugar conversion was determined on the basis of the amount of nonreacted glucose, fructose, and sucrose.

Isomerization experiments were carried out in magnetically stirred 10 mL glass vials heated in a temperature-controlled copper block. Five milliliters of a 10 wt % glucose (Aldrich) aqueous solution was added to 0.100 g of catalyst. The reaction was carried out at 383 K under autogenic pressure. Samples were taken at regular time intervals and analyzed by HPLC using a Metacarb 67C column.

RESULTS AND DISCUSSION

Catalyst Preparation and Characterization. Recently, we reported a new porous carbon-silica composite material (also denoted as CSM).[29] It contains a mesoporous silica framework, which is carefully filled with polyaromatic to graphite-like carbon (Figure 2). The porous carbon network is obtained by impregnation of a mesoporous silica such as MCM-41 with furfuryl alcohol (FA), followed by a heat induced polymerization and pyrolysis in inert atmosphere using a specific heating program. The perfect match of the impregnation and pore volume is crucial to obtain CSMs. Depending on the pyrolysis temperature, polyaromatic to graphite-like carbon was formed solely in the pores of the silica template.[29]

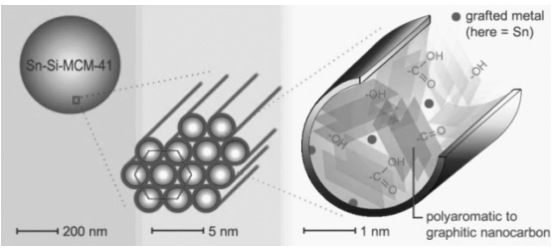

Figure 2. Schematic representation of the structure of a CSM catalyst at the various length scales.

Introduction of Lewis acidity is obtained by grafting Si-MCM-41 with Sn(IV) according to a previously described method.[34] It should be noted that a Lewis acid catalyst can also be obtained by addition of the proper Sn precursor into the synthesis gel.[38] The postsynthesis grafting was selected to ensure a controlled Sn accessibility. After grafting, the material was washed with isopropanol until less than 0.04 ppm Sn was analyzed in the washing solution. ICP-OES analysis shows a Sn content of 36.3 μmol g^{-1}, corresponding to 0.43 wt %, in the carbon-free Sn-Si-MCM-41 and a Sn:Si ratio of 1:460.

The 3d Sn XPS spectra of Sn-Si-CSM catalysts show a symmetric peak at a binding energy of 487.3 eV, indicative for Sn^{4+}. UV–vis diffuse reflectance of the hydrated Sn-Si-MCM-41 sample shows a broad absorption between 200 and 300 nm, which transforms after dehydration into two clear absorption features, at 210 and 260 nm, the former showing a clear intensity increase (Figure 3c). The high energy absorption band is due to a charge transfer process in isolated tetracoordinated tin(IV) oxide.[39,40] Earlier reports have shown that the unsaturated tetrahedral coordination sphere of such Sn species has an excellent water-tolerant Lewis acid property.[41] The low energy band is ascribed to charge transfer in fully hexacoordinated mono- to polymeric tin(IV) oxide and is expected not to contribute to the Lewis acid catalysis.[39,40] X-ray diffraction shows the retainment of the long-range order of the mesoporous Si-MCM-41 after grafting and no reflections due to crystalline SnO_2 (see Figure S3, Supporting Information).

The Lewis acid property of Sn was monitored with FT-IR after pyridine chemisorption. IR spectra were measured at various temperatures (Figure 3d). Vibrations characteristic of pyridine sorption on Lewis acid sites (denoted with L) were identified at 1455 (strong LA), 1615 (strong LA), and 1578 cm^{-1} (weak LA) in accordance with the literature.[34,42,43] Inspection of the spectra also reveals a very low content of Brønsted (indicated with B) acidity on Sn-grafted MCM-41.

Sn grafting has further no major impact on texture nor on morphology of the silica template. Both pure siliceous and Sn-grafted MCM-41 show a type I isotherm with a shift of the adsorption branch due to the larger pores (Figure 3b). As compared to the pure silica MCM-41, grafting only leads to a slight reduction in BET surface area and almost no reduction in pore size (DFT model). SEM images show spherical particles with a particle diameter of about 500 nm, similar to that of the parent MCM-41 material (Figure 3a).

Weak Brønsted acid groups are associated with the carbon framework of CSMs. The procedure to introduce (hydro) carbon into the silica pores has been described in detail elsewhere.[29] In short, furfuryl alcohol (FA) is impregnated in the pores of mesoporous silica, polymerized at elevated

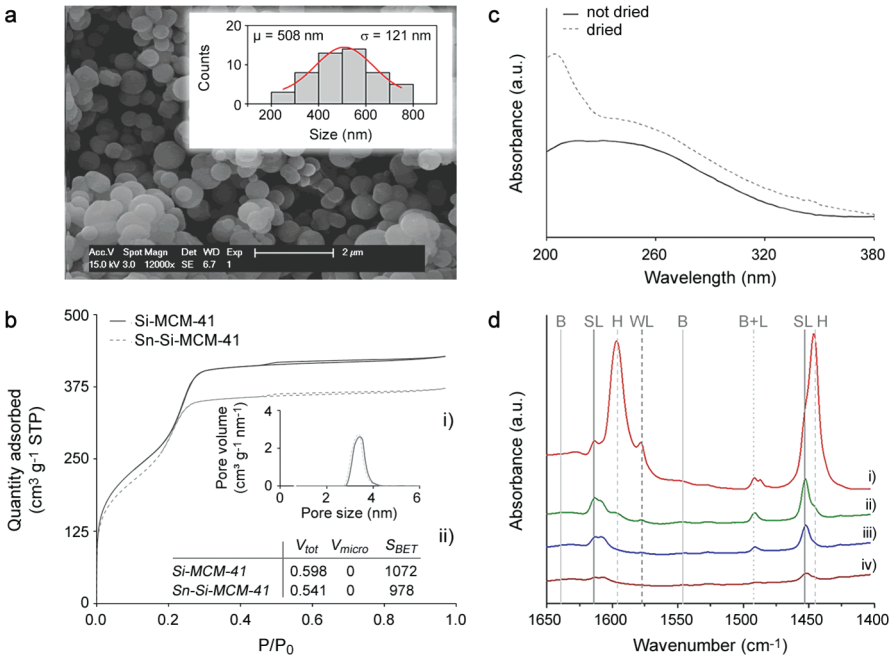

Figure 3. Physicochemical characteristics of the parent Sn-grafted spherical MCM-41: (a) Scanning electron micrograph. Inset: The average sphere diameter is estimated at 508 ± 121 nm (for $n = 50$). (b) N_2 sorption isotherms at liquid N_2 temperature. Inset: (i) Pore size distribution according to DFT method and (ii) texture data, V_{meso} and V_{micro} ($cm^3\ g^{-1}$) and BET ($m^2\ g^{-1}$). (c) Electronic spectrum in UV−Vis region, measured in diffuse reflectance mode. (d) FT-IR spectra in fingerprint domain after pyridine sorption and evacuation at (i) 323 K, (ii) 373 K, (iii) 423 K, and (iv) 473 K. Absorbance peaks characteristic of hydrogen bound pyridine (H), Brønsted (B), weak Lewis (WL), and strong Lewis (SL) sites are indicated.

Table 1. Amount of Carbon for a Given CSM (in wt %) As Obtained from TGA and CO_x Expulsion from TPD Experiments for Sn-Si-MCM-41-Derived Composites

entry	catalyst	FA (vol %)[a]	weight loss (wt %)[b]	CO_2[c]	CO[c]	total[c]
1	Sn-Si-CSM-773-21.6	75	21.6	0.04	0.48	0.52
2	Sn-Si-CSM-773-21.6/O_2 473 K	75	21.6	0.27	0.57	0.84
3	Sn-Si-CSM-773-18.3/O_2 573 K	75	18.3	0.56	0.64	1.20
4	Sn-Si-CSM-873-21.0	75	21.0	0.03	0.44	0.47
5	Sn-Si-CSM-873-20.3/O_2 473 K	75	20.3	0.03	0.37	0.40
6	Sn-Si-CSM-873-18.9/O_2 573 K	75	18.9	0.09	0.57	0.66
7	Sn-Si-CSM-973-21.0	75	21.0	0.02	0.40	0.42
8	Sn-Si-CSM-973-20.9/O_2 473 K	75	20.9	0.03	0.63	0.67
9	Sn-Si-CSM-973-19.8/O_2 573 K	75	19.8	0.08	0.66	0.74
10	Sn-Si-CSM-1073-20.7	75	20.7	0.03	0.25	0.28
11	Sn-Si-CSM-1273-20.6	75	20.5	0.02	0.09	0.12
12	Sn-Si-CSM-773-11.9	25	11.9	0.04	0.23	0.27
13	Sn-Si-CSM-773-16.4	50	16.4	0.05	0.38	0.42
14	Sn-Si-CSM-773-15.3/O_2 473 K	50	15.3	0.24	0.52	0.76
15	Sn-Si-CSM-773-14.9/O_2 573 K	50	14.9	0.48	0.54	1.02
16	Sn-Si-CSM-1173-15.7	50	15.7	0.02	0.31	0.33
17	Sn-Si-CSM-773-24.3	100	24.3	0.04	0.51	0.55

[a]Concentration of FA in the carbon precursor impregnation solution (vol %). [b]Total weight loss above 423 K according to a thermal gravimetric analysis in air (see Experimental Section). [c]Expressed in mmol g^{-1}.

temperature, and further heated at even higher temperatures. Mild pyrolysis of FA polymers is known to retain considerable amounts of oxygen in the resulting (hydro)carbon framework.[44] These atoms are present in various oxygen-containing surface species such as carbonyls, lactones, carboxylic anhydrides, and hydroxyl groups,[45] providing CSMs with weak Brønsted acidity. To further enhance the amount of surface oxygen groups, and thus the amount of weak Brønsted acid sites, a postsynthesis treatment was carried out under oxygen atmosphere at elevated temperature. Surface modification of carbon materials with oxidative gases like air, O_2, or CO_2 has been reported to increase the surface oxygen content.[46] Alternative chemical oxidation procedures, typically used for oxidizing carbon-like materials such as treatment with nitric or sulphuric acid,[47] are not suitable in this contribution, because they remove Sn from the silica support. The simple and cheap oxidation procedure in flowing oxygen gas was therefore preferred.

Temperature-programmed desorption, coupled with MS detection (TPD-MS), is a common tool to investigate the surface chemistry of carbonaceous materials.[29b,46,48,49] The oxidation degree as well as the nature and stability of the

dx.doi.org/10.1021/ja301678w | J. Am. Chem. Soc. 2012, 134, 10089−10101

oxygen-containing functional groups are determined by monitoring the evolution of CO_2 and CO gases during gradual heating of the samples in inert atmosphere. An illustration of representative gas evolutions is provided in the Supporting Information for selected CSM samples (Figure S4). The reactive surface oxygen content (in mmol g^{-1}, Table 1) of various CSM catalysts was calculated from the total evolution of CO_x during heating under inert He until 1273 K. Table 1 shows the influence of the composite composition and (post)synthesis procedure on the final surface oxygen content. First, the data demonstrate a gradual increase in total oxygen content with increasing carbon loadings (Table 1: entries 1, 12, 13, 17). For instance, 0.27 mmol g^{-1} CO_x was analyzed for composite Sn-Si-CSM-773-11.9 containing 11.9 wt % carbon, while 0.55 mmol g^{-1} CO_x was measured for Sn-Si-CSM-773-24.3 with 24.3 wt % carbon content. Second, the total oxygen content in the carbon part increases with a decreasing pyrolysis temperature (Table 1: entries 1, 4, 7, 10, 11). For instance, pyrolysis at 1273 K results in a composite from which 0.12 mmol g^{-1} CO_x evolves in the TPD experiment, while 0.47 mmol CO_x per gram evolves from samples pyrolyzed at 873 K. Finally, the postsynthesis oxidation treatment significantly increases the total oxygen content. This is clearly reflected in the higher release of CO and CO_2 during the TPD experiment (Table 1: compare entries 1 vs 2-3 and 7 vs 8-9).

The total amount of oxygen is proportional with the oxidation temperature of the post-treatment (Table 1): the highest CO_x losses, up to 1.20 mmol g^{-1}, are found for samples post-treated in oxygen at 573 K. Note that a profound carbon gasification takes place for samples treated in oxygen above 673 K, as confirmed by TGA under O_2 and by visual inspection (Figure 4): up to 70% of the carbon fraction is lost for a CSM

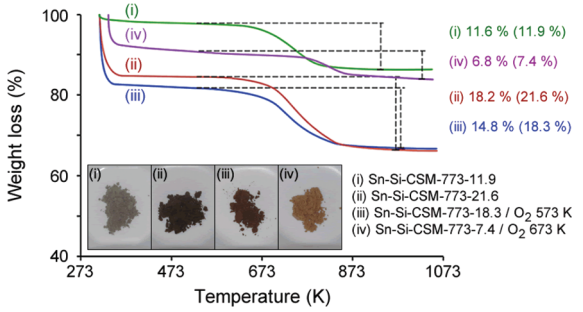

Figure 4. Thermal gravimetric analysis of samples Sn-Si-CSM-773-11.9 (i) and Sn-Si-CSM-773-21.6 before (ii) and after post-treatment in O_2 at 573 (iii) and 673 K (iv). The weight loss is indicated joint with the final carbon weight fraction of the composite in parentheses. True color photographs are shown in the inset.

pyrolized at 773 K and postoxidized at 673 K. Accordingly, a color change of the catalyst powder from typically dark brown for CSMs into light brown to white was clearly observed.

Oxygen-rich carbons have been considered to behave as weak Brønsted acidic materials.[47,50] Exact assignment of CO and CO_2, evolving at various temperatures, to specific functional groups proves difficult as peak temperatures are also affected by the heating rate, porosity, and geometry of the experimental system used.[51] In general terms, evolution of CO is ascribed to the presence of semiquinone and stable mono-oxygen species like carbonyls and phenols, while CO_2 is related to the presence of lactone or (anhydride) carboxylic groups.[48,51] The total amount of evolved CO (in particular from phenols and anhydrides) and CO_2 (from anhydrides and carboxylic acids) is thus a fair measure of the Brønsted acid content.[47a]

A selection of catalyst samples (Table 1, entries 1−3) was examined with XPS to confirm the carbon identity as a function of the pyrolysis temperature and post-treatment procedure. Figure 5a displays an overlay of the three spectra in the

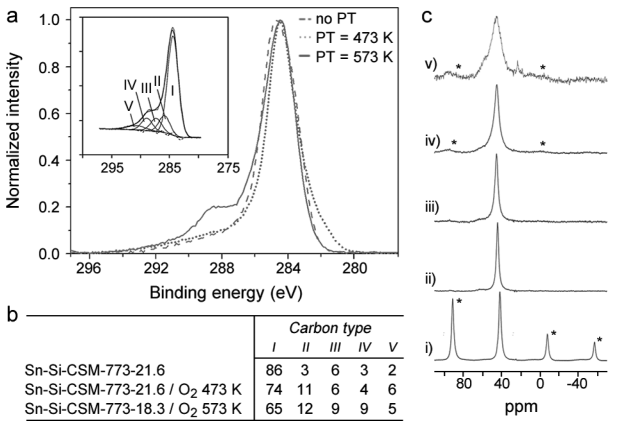

Figure 5. (a) XPS spectra and corresponding deconvolution of the C1s peak of Sn-Si-CSM-773-21.6 sample oxidized in a post synthesis treatment with O_2 at 473 or 573 K (inset). Carbon species: (I) graphitic, (II) phenol/ether/alcohol, (III) carbonyl/quinone, (IV) carboxyl/ester, and (V) shake up satellite peaks. (b) Relative amount of carbon species as obtained by deconvolution. PT = postsynthetic oxidation treatment in O_2. (c) ^{31}P NMR spectra of selected catalysts after chemisorption of trimethylphosphine oxide (TMPO): (i) reference TMPO (pure), (ii) Sn-Si-CSM-1173-15.7, (iii) Sn-Si-CSM-773-16.4, (iv) Sn-Si-CSM-773-24.3, and (v) Sn-Si-CSM-773-14.9/O_2 573 K. "*" denotes spinning side-bands.

characteristic binding energy region of C 1s. The shift in binding energy correlates with the type of oxygen−carbon group.[52] Deconvolution of the C 1s peak by pseudo-Voigt functions, such as illustrated in the inset of Figure 5a, allows the tentative assignment of various carbon species; graphitic carbon (I), phenol/ether/alcohol (II), carbonyl/quinone (III), and carboxyl/ester (IV) are distinguished. A fifth peak was assigned to shake up satellite peaks (V). For instance, the CSM sample Sn-Si-CSM-773-21.6, heated at 773 K, contains 12% oxidized carbon atoms (relative to the total of type I−IV). Post-treatment oxidation significantly increases the total amount of surface oxygen groups such as carbonyl, carboxylic, and phenolic carbons, at the expense of graphitic carbon. This trend is in fair agreement with the data of the TPD experiments in Table 1. About 22% of the carbon atoms are oxidized after postoxidation at 473 K, while the fraction increases to 32% after oxidation at 573 K (Figure 5b). The temperature of the post-treatment also affects the identity of the oxygen-containing carbon functionalities. Oxidation at 473 K significantly increases the amount of carbon present in phenolic groups, while carbonyl and carboxylic carbon atoms only slightly increase. Increasing the oxidation temperature to 573 K results in a pronounced increase of phenolic, carbonyl, and carboxylic carbon atoms.

In summary, the amount and nature of the oxygen-containing groups in the carbon part of the CSM composite, and thus of the weak Brønsted acidity, is controlled by three parameters: (i) carbon content, (ii) pyrolysis temperature, and (iii) postsynthetic oxidation treatment.

dx.doi.org/10.1021/ja301678w | J. Am. Chem. Soc. 2012, 134, 10089−10101

The acid strength of the solid acid CSM catalysts was probed using ^{31}P MAS NMR experiments on samples treated with TMPO (pK_B = 14.5) basic probe molecules. NMR spectra are illustrated in Figure 5c. ^{31}P chemical shifts of 40−70 ppm against the reference orthophosphoric acid have earlier been attributed to the presence of weak acidic oxygen-containing surface groups on carbonized material.[53] Chemical shifts increase with an increase of the acid strength with chemical shifts around 80 ppm and higher assigned to strong Brønsted acidity.[54]

Understoichiometric amounts of TMPO were used to analyze the strongest acid sites, because an excess of TMPO aggregates on the surface results in a sharp resonance signal at ca. 41 ppm, which interferes with the signal of TMPO adsorbed on weak acid sites.[53] None of the CSMs showed a signal at 41 ppm, indicating the absence of crystalline TMPO. Instead, CSMs show a strong signal at around 45 ppm.

An additional shoulder at 60 ppm indicative of slightly stronger acid sites appears for CSMs post-treated at 573 K. The broadening of the signal might be indicative of the increasing heterogeneity of acid sites in the sample. The sideband pattern is always weak and thus pointing to loosely bound TMPO molecules in agreement with the weak strength of the acid sites.[54,55] In summary, ^{31}P NMR signals of (thermally air-treated) CSMs are typical of TMPO adsorbed on weak Brønsted acid sites.[56]

Physical characterization of the composite CSMs was further carried out with SEM, nitrogen physisorption, and XRD. SEM images of the composites display unchanged spherical morphology with mean particle size of 500 nm. The long-range order of the porous silica template (XRD data not shown) was retained after deposition of carbon in agreement with earlier XRD data for similar CSMs.[29] Nitrogen sorption of CSM catalysts demonstrates the expected decrease in total pore volume and surface area upon filling the pores with (hydro)carbon material. Carbon deposition immediately introduces microporosity, while the total mesopore volume drops with increasing carbon content (Table 2).[29] For instance,

Table 2. Summary of the Textural Data of Various CSMs

catalyst	FA[a]	V_{tot}[b]	V_{micro}[c]	S_{BET}[d]
Si-MCM-41	0	0.598	0.000	1072
Sn-Si-MCM-41	0	0.541	0.000	978
Sn-Si-CSM-773-16.4	50	0.395	0.030	814
Sn-Si-CSM-773-21.6	75	0.267	0.120	561
Sn-Si-CSM-773-21.6/O_2 473 K	75	0.275	0.119	561
Sn-Si-CSM-773-18.3/O_2 573 K	75	0.273	0.110	559
Sn-Si-CSM-773-24.3	100	0.205	0.205	414

[a]Concentration of furfuryl alcohol (FA) in impregnation solution (vol %). [b]Total pore volume derived from the isotherm log plot ($cm^3\ g^{-1}$). Determined by a linear fit in the pressure region P/P_0 0.4−0.7. [c]Micropore volume as determined by t-plot analysis ($cm^3\ g^{-1}$). Determined by a linear fit in the pressure region P/P_0 0.05−0.16. [d]Specific BET surface area ($m^2\ g^{-1}$). Determined by a linear fit in the pressure region P/P_0 0.05−0.3.

introducing 16.4 wt % (hydro)carbon in Sn-MCM-41 lowers the mesopore volume from 0.541 to 0.395 $cm^3\ g^{-1}$, while 0.030 $cm^3\ g^{-1}$ micropore volume was generated. Introducing more carbon, 21.6 wt %, shifts the material into a biporous composite with comparable meso- and micropore volume, 0.147 and 0.120 $cm^3\ g^{-1}$, respectively. An exclusively microporous material with 0.205 $cm^3\ g^{-1}$ micropore volume is obtained after filling the parent Sn-MCM-41 with 24.3 wt % (hydro)carbon. In earlier reports, we noticed that the micropores exert shape selective behavior when prepared at high pyrolysis temperatures.[29] Pore volume and surface area remain nearly unaffected by the applied oxidation post-treatment for temperatures below 573 K (see Table 2). Higher oxidation pretreatment temperatures however reintroduce mesoporosity at the expense of microporosity as a result of carbon removal due to gasification (data not shown).

Conversion of DHA to Alkyl Lactate in Alcoholic Solvent. Conversion of DHA in ethanol was performed using various reference catalysts. Acid type and strength are expected to be crucial parameters toward the final product selectivity taking into account the proposed reaction network of Figure 1. As a consequence of that, both strong and weak Brønsted acid catalysts were examined (Table 3). A strong Brønsted acid

Table 3. Overview of Catalytic Conversion of DHA in Ethanol[a]

entry	catalyst	X (%)	S_{ELA} (%)	TON[b]
1	Nafion NR50	92	0	n/a
2	Amberlite IRC-50	22	0	n/a
3	Sn-Si-MCM-41	26	90	71
4	Si-CSM-1073-22.3	5	25	n/a
5	Si-CSM-773-25.5/SO_3H	36	10	n/a
6	Sn-Si-CSM-773-11.9	39	94	119
7	Sn-Si-CSM-773-16.4	60	97	224
8	Sn-Si-CSM-773-21.6	69	98	260
9	Sn-Si-CSM-773-24.3	88	99	325
10	Sn-Si-CSM-673-17.1	29	95	129
11	Sn-Si-CSM-973-15.7	62	98	228
12	Sn-Si-CSM-1173-15.4	40	96	165
13	Sn-Si-CSM-773-15.3/O_2 473 K	86	98	313
14	Sn-Si-CSM-773-14.9/O_2 573 K	100	100	346
15	Sn-Si-CSM-773-6.4/O_2 673 K	71	98	208

[a]Reaction conditions: 5 mL of ethanol, 0.1 g of catalyst, 0.09 g of DHA, 1 atm N_2, 363 K, 6 h. [b]Total turnover number after 6 h (mol $DHA_{converted}$ per mol Sn).

catalyst such as the sulfonic acid containing Nafion NR50 demonstrates a high conversion of DHA (92%), but no ethyl lactate was formed (Table 3: entry 1). Instead, DHA is exclusively converted into acetal products of PAL. A similar observation was made with a sulfonated CSM catalyst (Table 3: entry 5), prepared according to Peng et al.;[57] activity is moderate (36% conversion) and selectivity to ethyl lactate is low (9%) due to competitive acetalization of PAL (Figure 1). Amberlite IRC-50, a polystyrene resin containing carboxylic groups, was chosen to benchmark weaker Brønsted acidity. No trace of ethyl lactate nor acetal products was formed (Table 3: entry 2), while PAL was formed exclusively at 22% DHA conversion. This observation clearly demonstrates the importance of weak Brønsted acid sites in the conversion of DHA to PAL. A similar observation was found for Si-CSM-1073-22.3, a CSM without Lewis acidity (Table 3: entry 4). The selective formation of PAL again confirms the ability of weak Brønsted acids to catalyze DHA isomerization, GLY dehydration, and rearrangement into PAL, but not to assist the conversion of PAL into ethyl lactate. In agreement with previous reports, Lewis acid catalysts such as Sn grafted MCM-41 (Table 3: entry 3) are capable of converting DHA into ethyl

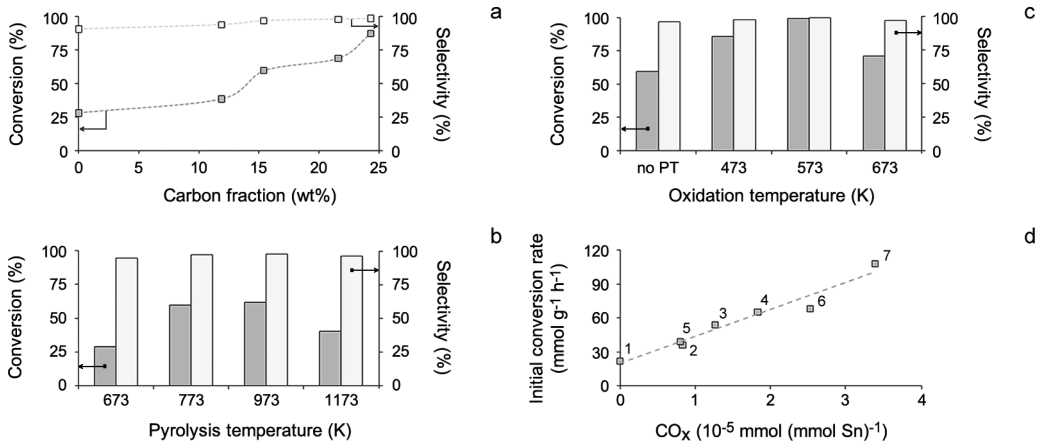

Figure 6. Overview of the influence of synthesis parameters on the overall DHA conversion and selectivity toward ethyl lactate after 6 h of reaction. Conditions are according to those of Table 3: (a) varying carbon deposition using Sn-Si-CSM-773-Y; (b) varying pyrolysis temperature using Sn-Si-CSM-X-Y catalysts prepared from a 50 V% FA precursor solution; (c) varying post-treating temperature (8 h in O_2) using Sn-Si-CSM-773-16.4 as parent catalyst; (dark gray) conversion of DHA (light gray) selectivity toward ELA; and (d) plot of initial conversion rate (the kinetic profiles are not shown) as a function of total evolved CO_x during TPD (data taken from Table 1). The labels of the data points correspond to the catalyst numbers in Table S1 in the Supporting Information. The dashed line is a guide to the eye.

lactate with high selectivity, albeit at a low conversion rate. We ascribe the low activity to the low content of residual Brønsted acidic silanols after surface grafting with Sn(IV). As was reported recently, direct incorporation of Sn in silica instead of Sn grafting generates weak Brønsted acidity, providing the catalyst with a higher overall activity.[20]

Because only traces of PAL are analyzed in the reaction product mixtures, its formation can be considered rate determining. Therefore, we anticipate to be able to increase the formation rate of ethyl lactate by increasing the amount of weak Brønsted acid sites in the catalyst. Hence, the reference Sn-Si-MCM-41 catalyst was loaded with various amounts of oxygen-rich carbon, optionally undergoing an additional treatment in oxygen atmosphere at various temperatures to further increase the weak Brønsted acid content. A series of Sn-grafted CSMs with varying carbon content, pyrolysis temperature, and oxygen treatments was critically examined. The hybrid materials were prepared from the same batch of Sn grafted MCM-41. The amount of carbon deposited inside the pores was varied by changing the furfuryl alcohol (FA) concentration (see Table 1) of the impregnation solution.[29]

A clear increase in activity is observed for the series Sn-Si-CSM-773-Y catalysts with increasing carbon content from 0 to 24.3 wt %, corresponding to a 0−100 vol % FA precursor impregnation solution (Table 3: entries 3, 6−9; Figure 6a). For example, the parent carbon-free Sn-Si-MCM-41 shows 26% of DHA conversion after 6 h, while the conversion is almost 90% for Sn-Si-CSM-773-24.3 containing 24 wt % of oxidized (hydro)carbon (Table 3: entry 9). As the number of weak Brønsted acid sites runs parallel with the amount of (hydro) carbon (vide supra), the hypothesis of triggering the first (rate-determining) step in the reaction mechanism seems valid. On the basis of the kinetic data, a 3-fold initial reaction rate is achieved due to the presence of oxidized carbon: the rate increases from 22 to 65 μmol min^{-1} g^{-1} after deposition of a maximum of 24 wt % of carbon. Likewise, the corresponding initial turnover frequencies (TOF based on Sn) were calculated and determined at 41 and 142 h^{-1}, respectively. In summary, the large increase of the initial conversion rate accords to acceleration of the rate-determining first step, that is, the conversion of DHA to PAL, due to the presence of oxygen-containing surface functional groups with mild Brønsted acid properties.

In addition to the enhancement of the initial rate, carbon-containing catalysts also show a very stable conversion, as demonstrated by the higher turnover numbers after 6 h (Table 3). In the formation of ethyl lactate, Sn in Sn-Si-CSM-773-24.3 turns over about 325 times, which is almost 5 times higher than the parent carbon-free Sn-Si-MCM-41 for the same reaction time (Table 3: compare entries 3 and 9). Also, the ethyl lactate selectivity slightly increases with the carbon content (Table 3: entries 3, 6−9). While it was 90% for the parent Sn-Si-MCM-41, values almost as high as 99% were analyzed for the carbon-rich Sn-Si-CSM-773-24.3. The acid strength of the pool of oxygen-containing functional groups is thus sufficient to encourage PAL formation in the first step of the mechanism, but interestingly it is not strong enough to trigger the unwanted acetal formation.

The influence of the pyrolysis temperature is illustrated in Figure 6b and Table 3 (entries 7, 10−12) for Sn-Si-CSM-X-Y samples containing about 15−16 wt % carbon (X); the pyrolysis temperature is varied between 673 and 1173 K. Maximum activity was observed for samples heated in inert He at temperatures between 773 and 973 K. Activity significantly drops with further increase of the pyrolysis temperature. This observation is explained by the drop of oxygen content in the carbon part with increasing pyrolysis temperature in accordance with the aforementioned TPD/MS and TGA study in Table 1. Pyrolysis below 773 K results in incomplete carbonization of the FA polymer, leaving mainly cyclic ether functional groups in the (hydro)carbon matrix, which have no Brønsted acid properties.

Because the weak Brønsted acid content determines the overall reaction rate, new ways to further increase its number were explored. Sn-Si-CSM-773-16.4 samples were therefore subjected to a quick heat treatment under flowing O_2 at various temperatures before catalysis. Its positive effect on the catalytic performance is apparent from the data in Table 3 (entries 7, 13, 14) and Figure 6c. The oxidation cure clearly promotes the selective conversion of trioses to ethyl lactate. The lactate yield increases from 60% with the untreated sample to 100% for the catalyst treated at 573 K. The initial DHA conversion rate in

the presence of Sn-Si-CSM-773-14.9/O_2 573 K amounts to 149 μmol min^{-1} g^{-1}, corresponding to a TOF of 289 h^{-1}. This value is considerably higher than that of bare Sn-Si-MCM-41 and nonoxidized Sn-Si-CSM-773-16.4, 22 and 54 μmol min^{-1} g^{-1}, respectively. The significant rate enhancement accords with the increased levels of weak Brønsted acid functional groups in the carbon matrix (see Table 1). The selectivity remains unchanged at around 99%, in agreement with the low strength of the Brønsted acid sites (see ^{31}P NMR study).

At a postoxidation at 673 K, the activity drops significantly. The conversion drop (to 71%) is due to carbon gasification during the postsynthesis pretreatment, leaving almost no residual oxidized carbon (6.4 wt %). Nevertheless, conversion remains well above the values obtained with bare Sn-Si-MCM-41 and Sn-Si-SM-773-11.9 catalyst, that is, 26% and 39%, respectively (Table 3: entries 3 and 6). Despite the low content of carbon, the remaining fraction holds at least a significant oxygen density, as it was oxidized at a higher temperature.

Figure 6d plots the initial triose conversion rates of an arbitrary set of CSM catalysts as a function of the total CO_x content released during temperature-programmed desorption. The kinetic data were obtained from conversion evolution plots in time at isoconversion points of about 10% (see the Supporting Information), while the content of weak Brønsted acid functional groups was derived from the TPD data, as summarized in Table 1. This plot demonstrates a clear correlation between the initial conversion rate and the amount of weak Brønsted acids. The relationship validates our initial hypothesis to fasten the first rate-determining step by the addition of weak Brønsted acids; the more CO_x that evolves in TPD and thus the more acids present for a given Sn content, the faster is the reaction rate.

To illustrate the catalytic stability at incomplete conversion, a nonoxidized catalyst, Sn-Si-CSM-773-24.3, was reused several times for DHA conversion into ethyl lactate in ethanol (Figure 7: dark gray). Conversion after 6 h, 88%, and selectivity, +99%,

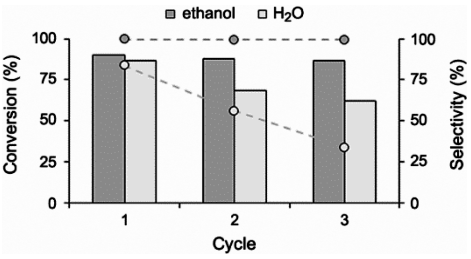

Figure 7. Recycling test of catalysts using Sn-Si-CSM-773-24.3 (dark gray) in ethanol and (light gray) water. The *Y*-axes present the conversion of DHA (bars) and selectivity (circles) toward ethyl lactate (in ethanol) and lactic acid (in water).

remain unchanged in the reruns. Furthermore, no DHA conversion occurred in the filtrate after separating the catalyst. In accordance, ICP-OES analysis of the filtrate after reaction in ethanol indicates very low Sn leaching.

An average of 0.19 ppm Sn was analyzed in the reaction solutions, corresponding to a loss of 0.3% of the total amount of tin originally present.

The synthesis of long chain alkyl lactates was further pursued to broaden the scope of the bifunctional (weak Brønsted acid–Lewis acid) CSMs. Long chain lactate esters are of high importance in healthcare and cosmetic industrial applications.[13] One of the best CSM catalysts, Sn-Si-CSM-773-24.3, was selected to convert DHA into the corresponding lactate ester in tetradecanol.

A limited yield of 20% was observed (Table 4: entry 5), likely because of steric constraints of the large alcohol molecule in the microporous network of Sn-Si-CSM-773-24.3 (see Table 2). Usage of a biporous CSMs such as Sn-Si-CSM-773-16.4, containing less intraporous carbon (see Table 2), results in a substantial tetradecyl lactate yield of 54% (Table 4: compare entries 4 and 5). This example nicely illustrates the flexibility of CSMs to readily adapt the pore architecture at will. Fair yields were also obtained with other long alkyl chain alcohols. Octyl lactate, for instance, can be produced from DHA in a single step with an excellent yield of 83% (Table 4: entries 1–3).

Table 4. DHA Conversion in Various Alcoholic Solvents[a]

entry	catalyst	solvent	Y_{ALA} (%)[b]
1	Sn-Si-CSM-773-16.4	octanol	83
2	Sn-Si-CSM-773-16.4	decanol	67
3	Sn-Si-CSM-773-16.4	dodecanol	53
4	Sn-Si-CSM-773-16.4	tetradecanol	54
5	Sn-Si-CSM-773-24.3	tetradecanol	20

[a]Reaction conditions: 5 mL of alcohol, 0.1 g of catalyst, 0.09 g of DHA, 363 K, 6 h. [b]Y_{ALA} = alkyl lactate yield as determined by GC-analysis using ECN-based calculations.[37]

Conversion of DHA to Lactic Acid in Water. The catalytic reaction was also carried out in water to produce lactic acid according to the scheme in Figure 1. Again, an increase of DHA conversion rate is observed with increasing carbon content. For instance, after 6 h, the conversion increases from 59% to 87% (Table 5: entries 2 vs 3-4). Although the effect is less pronounced as compared to the catalytic tests in alcoholic media, preoxidation of the carbon component clearly further increases DHA conversion (92%) and lactic acid yield (77%) (Table 5: entries 6 vs 3).

Table 5. Conversion of DHA in Water Solvent[a]

entry	catalyst	X_{DHA}[b]	S_{LA}[b]
1	Si-MCM-41	33	19
2	Sn-Si-MCM-41	59	39
3	Sn-Si-CSM-773-21.6	87	79
4	Sn-Si-CSM-773-24.3	87	78
5	Sn-Si-CSM-873-21.0	87	75
6	Sn-Si-CSM-773-18.3/O_2 573 K	92	83

[a]Reaction conditions: 5 mL of H_2O, 0.1 g of catalyst, 0.09 g of DHA, 383 K, 6 h. [b]As expressed in %.

Recycling experiments of the CSM catalysts in water showed a strong conversion drop (−18%) after the first recycling. Deactivation, although less pronounced, continues in the second recycling (−6%) (Figure 7). ICP-OES analysis showed amplified Sn leaching in aqueous solvent as compared to alcoholic media; the reaction solution contains an average of 0.46 ppm Sn corresponding to a loss of 0.66% of the initial Sn content. Additionally, the solution of the experiment with catalyst Sn-Si-CSM-773-21.6 was tested for residual activity of leached Sn species in the conversion of an additional aliquot of DHA after removal of the catalyst. The additional yield of lactic acid was determined at 11%. This value is only slightly higher as compared to the reference catalyst Si-MCM-41 (6%) without Sn, but is considerably lower when compared to soluble Sn

dx.doi.org/10.1021/ja301678w | J. Am. Chem. Soc. 2012, 134, 10089–10101

species.[17] The drop in activity when reusing the catalyst therefore seems unaccounted for solely by metal leaching. As a weight increase of the catalyst was consistently measured after each recycle, deactivation is likely explained due to carbonaceous deposition. Its identity could not be determined unambiguously against the carbon framework already present in CSMs.

Alkyl Lactate from Sugars Composed of Hexoses in Alcohol Solvent. The direct formation of alkyl lactates from common sugars such as sucrose, glucose, and fructose was also evaluated. The industrial relevance is significantly larger as the sugars are a sustainable, abundant, and low cost substrate. The reaction pathway is obviously more complex because of the occurrence of additional reaction types such as hydrolysis, isomerization, and retro-aldol reactions.[59] For instance, retro-aldol is required to cleave fructose into DHA and GLY. After isomerizing DHA into GLY, alkyl lactates and lactic acid are formed according to the same reaction network described above (see Figure 1). The use of sucrose entails an additional cleavage to fructose and glucose before retro-aldol cleavage. The latter reaction is further complicated in alcoholic solvent because of formation of less reactive alkyl glycosides. In view of selective lactate formation, fast isomerization of glucose to fructose is a necessity, because otherwise retro-aldol of glucose likely occurs yielding erythrose and glycolaldehyde. The catalytic data for the conversion of mono- and disaccharides in methanol to methyl lactate in the presence of Sn containing CSMs are presented in Table 6.

Table 6. Conversion of Mono- and Disaccharides to Methyl Lactate[a]

entry	catalyst	substrate	Y_{MLA}
1	Blank	sucrose	2
2	$SnCl_4 \cdot 5H_2O$	sucrose	26
3	Sn-Si-MCM-41	sucrose	18
4	Sn-Si-CSM-773−20.4	sucrose	45
5	Sn-Si-CSM-773−20.4	fructose	32
6	Sn-Si-CSM-773−20.4	glucose	17
7	Sn-Si-CSM-773-16.8/O_2 573 K	sucrose	18

[a]Reaction conditions: 428 K, 20 h, 6.0 g of methanol, 0.16 g of catalyst, 0.12 g of naphthalene, 0.225 g of saccharide. Methyl lactate yields expressed in molar percentages. Sugar conversion is always larger than 95% in entries 2−7.

No methyl lactate is formed from sucrose without catalyst (entry 1). The carbon-free Sn-Si-MCM-41 converts less sucrose into methyl lactate than does the homogeneous tin salt (18% vs 26% yield; entries 2 vs 3). In accordance with earlier findings in this report, the presence of weak Brønsted acidity (here, from oxidized carbon) in Sn-containing CSMs yields more methyl lactate; for example, 45% methyl lactate yield was obtained in the presence of Sn-Si-CSM−FA-773-20.4 (entry 4). Surprisingly lower methyl lactate yields were formed with fructose and glucose when compared to that of sucrose (compare entries 5 and 6 with 4). This observation is in agreement with an earlier report using Sn-Beta zeolite.[25] Higher contents of Brønsted acidity in the catalyst are, however, detrimental for the selectivity (entry 7).

The reaction network for the conversion of sucrose in methanol is obviously more complex than that for the conversion of trioses. Acid-catalyzed methanolysis of sucrose leads to fructose and methyl acetal of glucose, while hydrolysis leads to fructose and glucose. Fructose and glucose may undergo a multifold of reactions. When present in methanol in the presence of strong Brønsted acidity, their concentration is in equilibrium with the corresponding methyl fructosides and glycosides. These acetals are nonreducing sugars and are therefore unreactive against retro-aldol chemistry. The product mixture of entry 4, for instance, contains 1.2 mol % of such methylated sugars. When the catalyst contains a high content of Brønsted acidity, as in case of the postoxidized CSM in entry 7, the methyl lactate yield drops remarkably from 45% to 18% (Table 6: entries 4 vs 7), while methylated sugars become indeed the dominant product (about 27% yield).

Although it is not yet understood whether catalysis is involved or not, open forms of fructose and glucose, the hydrolysis products of sucrose, undergo retro-aldol reaction in the reaction conditions. Retro-aldol of fructose yields GLY and DHA, which further transform into the desired methyl lactate (45% yield, entry 4) through the formation of PAL (1% yield) (see Figure 1), while retro-aldol of glucose, an aldose instead of a ketose, yields glycolaldehyde and erythrose. Starting with sucrose, we evidenced the presence of glycolaldehyde dimethyl acetal (2% yield) and methyl glycolate (1% yield), but also C4 containing oxygenates such as methyl vinylglycolate (MVG, 2%), methyl-2-hydroxybutanoate (MHB, 3%), and methyl-4-methoxy-2-hydroxybutanoate (MMHB, 4%) were identified. The first C2 molecules are clearly attributed to the formation of glycolaldehyde, while the C4 molecules probably originate from the aldotetrose. In total, more than 10 mol % of sucrose underwent this reaction pathway (via glucose). The proposed mechanism is substantiated by the product analysis of a catalytic experiment using erythrose as feed instead of sucrose. In the reaction conditions of Table 6, erythrose is fully converted (+99%), and 21% MMHB, 6% MVG, and 6% of MHB are found. The formation mechanism likely follows a retro-Michael reaction. A more detailed proposal of the reaction scheme is provided in the Supporting Information (Figure S11).

Methyl lactate thus originates from fructose according to the proposed reaction scheme. This is further emphasized by the higher yield of methyl lactate using fructose (entry 5, 32%) as compared to glucose (entry 6, 17%) in Table 6. To increase methyl lactate yield, the competitive isomerization reaction should be slow with fructose, while methyl lactate from glucose entails a high isomerization activity. Recent work has proven this Lobry−de Bruyn−van Ekenstein type of transformation in the presence of Lewis acid Sn-containing catalysts.[40] Sn-containing CSM catalysts in this work were therefore tested for their ability to isomerize glucose. Isomerization at 383 K occurs, but its rate (per catalyst weight) was lower than reported values with Sn-Beta; for instance, a fructose yield of 5% was obtained after 2 h reaction with Sn-Si-CSM-773-16.4, while Sn-Beta yields 31%, within 30 min.[40b] Sn-containing CSMs are therefore good catalysts for converting fructose to methyl lactate, while the aldose/ketose isomerization ability currently seems insufficient to obtain a selective glucose conversion.

Despite the higher methyl lactate yield from fructose as compared to glucose, sucrose remains the substrate of choice (see entry 4). Sucrose is a disaccharide of glucose and fructose joined by an $\alpha,\beta(1\rightarrow 2)$glycosidic linkage, from the hemiacetal −OH groups of α-D-glucose and β-D-fructose. Sucrose does not contain a hemiacetal linkage and is therefore less reactive. This is, for instance, reflected in the thermal stability of sucrose, 462 K, when compared to glucose and fructose, 443 and 410 K,

respectively.[58] In this respect, the use of sucrose allows the gradual release of monosaccharides in the reaction solution, minimizing undesirable parallel reaction pathways such as fructose dehydration to hydroxymethyl furfural (HMF) and other intermediates.[59−64] Traces of methyl levulinate and HMF were analyzed, together with HMF derived acetals such as, 2-dimethoxymethyl-5-methoxymethyl furan (DMMF) and 5-hydroxymethyl-2-dimethoxymethyl furan (DHMF), but they only account for a total of 0.3% yield (in case of entry 4). A substantial increase in HMF and its acetals and methyl levulinate was noticed with a combined yield of 12% in the presence of a catalyst with high Brønsted acid density, such as in Sn-Si-CSM-773-16.8/O_2 573 K (entry 7).

■ CONCLUSIONS

We have demonstrated that specially designed and fine-tuned carbon-silica composite (CSM) catalysts are capable of selectively converting sugars (such as trioses and hexoses) into lactic acid and various alkyl lactates. The framework of the composite consists of a porous silica template, filled with pyrolyzed (hydro)carbon, and contains both Lewis and weak Brønsted acid sites. Lewis acid sites were introduced, prior to carbon filling, by grafting the silica surface with Sn(IV), while the surface functional groups like phenols, anhydrides, and carboxylic acids in the carbon framework deliver weak Brønsted acids. The presence of both acid site types is a prerequisite to a fast and selective conversion of trioses into alkyl lactates and lactic acid. The bifunctional design was focused as to maximize alkyl lactate and lactic acid formation (rate) by balancing the number of weak Brønsted acid sites for a given content of Sn. The number of Brønsted acid sites and their strength were controlled by the carbon deposition content, the pyrolysis temperature, and thermal post-treatment. Strong Brønsted acidity should be avoided as they trigger unwanted competitive reactions. A 7-fold increase of the reaction rate for triose conversion was achieved after carefully balancing the two acid types: the initial TOF (based on Sn) was increased from 41 to 289 h^{-1}, while a quantitative conversion of triose to ethyl lactate in ethanol was achieved. This activity is among the highest values reported to date.[19,20] Tailoring the pore size of CSMs allows the high yield synthesis of useful amphiphilic alkyl lactates such as decyl lactate from sugars and long chain alcohols. The bifunctional catalytic concept was finally proven for the one-pot conversion of hexose sugars into alkyl lactates in alcohol. Despite the complex reaction network, a considerable alkyl lactate yield was obtained from sucrose. Research is in progress to further fine-tune the catalyst to improve the alkyl lactate yield from cheap sucrose feeds, while other cascade reactions requiring multifunctional catalysis are waiting to be explored with porous carbon-silica composites.

■ ASSOCIATED CONTENT

Supporting Information

Characterization of catalysts (ICP-OES, Sn-XPS, XRD, SEM, and TPD-MS), analysis of chemicals (GC and HPLC chromatograms), kinetic study, and proposed reaction scheme. This material is available free of charge via the Internet at http://pubs.acs.org.

■ AUTHOR INFORMATION

Corresponding Author

bert.sels@biw.kuleuven.be

Author Contributions

‖These authors contributed equally.

Notes

The authors declare no competing financial interest.

■ ACKNOWLEDGMENTS

We thank the Belgian Science Policy for providing support. The grant associated with its "interuniversity attraction poles" (IAP) program made this Ph.D. research topic possible. M.D. acknowledges "FWO Vlaanderen" (Grant 1.1.955.10N) for financial support. The Research Council of the K.U. Leuven (IDO - 3E090504) is also gratefully acknowledged. We thank the long-term structural funding of the Flemish government (Methusalem). We are grateful to Sofie Mannaerts for her help with ICP analysis, Kristof Houthoofd for his assistance in ^{31}P NMR, Elke Verheyen for her support in the determination of the PSD (DFT model), and Roselinde Ooms.

■ REFERENCES

(1) (a) Corma, A.; Iborra, S.; Velty, A. *Chem. Rev.* **2007**, *107*, 2411−2502. (b) Ragauskas, A. J.; Williams, C. K.; Davison, B. H.; Britovsek, G.; Cairney, J.; Eckert, C. A.; Frederick, W. J.; Hallett, J. P.; Leak, D. J.; Liotta, C. L.; Mielenz, J. R.; Murphy, R.; Templer, R.; Tschaplinski, T. *Science* **2006**, *311*, 484−489. (c) Bozell, J. J.; Petersen, G. R. *Green Chem.* **2010**, *12*, 539−554. (d) Van de Vyver, S.; Geboers, J.; Jacobs, P. A.; Sels, B. F. *ChemCatChem* **2011**, *3*, 82−94. (e) Rose, M.; Palkovits, R. *Macromol. Rapid Commun.* **2011**, *32*, 1299−1311. (f) Gallezot, P. *Chem. Soc. Rev.* **2012**, *41*, 1538−1558.

(2) Alakomi, H. L.; Skytta, E.; Saarela, M.; Mattila-Sandholm, T.; Latva-Kala, K.; Helander, I. M. *Appl. Environ. Microbiol.* **2000**, *66*, 2001−2005.

(3) Datta, R.; Henry, M. *J. Chem. Technol. Biotechnol.* **2006**, *81*, 1119−1129.

(4) PlasticsEurope Market Research Group (PEMRG). Plastics - the Facts 2011: An analysis of European plastics production, demand and recovery for 2010. November 4, 2011; http://www.plasticseurope.org/information-centre/publications-test.aspx (accessed Jan 2, 2012).

(5) Shah, A. A.; Hasan, F.; Hameed, A.; Ahmed, S. *Biotechnol. Adv.* **2008**, *26*, 246−265.

(6) Nampoothiri, K. M.; Nair, N. R.; John, R. P. *Bioresour. Technol.* **2010**, *101*, 8493−8501.

(7) (a) Drumright, R. E.; Gruber, P. R.; Henton, D. E. *Adv. Mater.* **2000**, *12*, 1841−1846. (b) Kamber, N. E.; Jeong, W.; Waymouth, R. M.; Pratt, R. C.; Lohmeijer, B. G. G.; Hedrick, J. L. *Chem. Rev.* **2007**, *107*, 5813−5840. (c) Dechy-Cabaret, O.; Martin-Vaca, B.; Bourissou, D. *Chem. Rev.* **2004**, *104*, 6147−6176. (d) Auras, R. A.; Lim, L.-T.; Selke, S. E. M.; Tsuji, H. *Poly(Lactic Acid): Synthesis, Structures, Properties, Processing, and Applications*; J. Wiley & Sons: Hoboken, 2010.

(8) European Bioplastics. European Bioplastics - Driving the evolution of plastics; http://en.european-bioplastics.org/multimedia/ (accessed Jan 2, 2012).

(9) Shen, L.; Worrell, E.; Patel, M. *Biofuels, Bioprod. Biorefin.* **2010**, *4*, 25−40.

(10) (a) Chamberlain, B. M.; Cheng, M.; Moore, D. R.; Ovitt, T. M.; Lobkovsky, E. B.; Coates, G. W. *J. Am. Chem. Soc.* **2001**, *123*, 3229−3238. (b) Jing, F.; Hillmyer, M. A. *J. Am. Chem. Soc.* **2008**, *130*, 13826−13827. (c) Jones, G.; Jenkins, S. J. *J. Am. Chem. Soc.* **2008**, *130*, 14483−14492. (d) Serrano-Ruiz, J. C.; Dumesic, J. *Green Chem.* **2010**, *11*, 1101−1104. (e) Katryniok, B.; Paul, S.; Dumeignil, F. *Green Chem.* **2010**, *12*, 1910−1913. (f) Inkinen, S.; Hakkarainen, M.; Albertsson, A.-C.; Södergård, A. *Biomacromolecules* **2011**, *12*, 523−532.

(11) (a) Zhang, J.; Zhao, Y.; Pan, M.; Feng, X.; Ji, W.; Au, C.-T. *ACS Catal.* **2010**, *1*, 32−41. (b) Cortright, R. D.; Sanchez-Castillo, M.; Dumesic, J. A. *Appl. Catal. B-Environ.* **2002**, *39*, 353−359.

(12) (a) Pereira, C. S. M.; Silva, V. M. T. M.; Rodrigues, A. E. *Green Chem.* **2011**, *13*, 2658−2671. (b) Beeson, W. H.; Rockhill, H. T. CA Patent 2,615,630, June 26, 2008.
(13) (a) Kreps, S. I. U.S. Patent 3,098,795, July 23, 1963. (b) EWG's Skin Deep Cosmetics Database. http://www.ewg.org/skindeep/ (accessed Feb 3, 2012).
(14) (a) John, R. P.; Nampoothiri, K. M.; Pandey, A. *Appl. Microbiol. Biotechnol.* **2007**, *74*, 524−534. (b) Okano, K.; Tanaka, T.; Ogino, C.; Fukuda, H.; Kondo, A. *Appl. Microbiol. Biotechnol.* **2010**, *85*, 413−423.
(15) Abdel-Rahman, M. A.; Tashiro, Y.; Sonomoto, K. *J. Biotechnol.* **2011**, *156*, 286−301.
(16) Wasewar, K. L.; Yawalkar, A. A.; Moulijn, J. A.; Pangarkar, V. G. *Ind. Eng. Chem. Res.* **2004**, *43*, 5969−5982.
(17) Hayashi, Y.; Sasaki, Y. *Chem. Commun.* **2005**, 2716−2718.
(18) (a) Janssen, K. P. F.; Paul, J. S.; Sels, B. F.; Jacobs, P. A. *Stud. Surf. Sci. Catal.* **2007**, *170B*, 1222−1227. (b) Pescarmona, P. P.; Janssen, K. P. F.; Stroobants, C.; Molle, B.; Paul, J. S.; Jacobs, P. A.; Sels, B. F. *Top. Catal.* **2010**, *53*, 77−85. (c) West, R. M.; Holm, M. S.; Saravanamurugan, S.; Xiong, J.; Beversdorf, Z.; Taarning, E.; Christensen, C. H. *J. Catal.* **2010**, *269*, 122−130. (d) Rasrendra, C. B.; Fachri, B. A.; Gusti, I.; Makertihartha, B. N.; Adisasmito, S.; Heeres, H. J. *ChemSusChem* **2011**, *4*, 768−777. (e) Wang, J. C.; Masui, Y.; Onaka, M. *Appl. Catal. B-Environ.* **2011**, *107*, 135−139.
(19) (a) Taarning, E.; Saravanamurugan, S.; Holm, M. S.; Xiong, J.; West, R. M.; Christensen, C. H. *ChemSusChem* **2009**, *2*, 625−627. (b) Pescarmona, P. P.; Janssen, K. P. F.; Delaet, C.; Stroobants, C.; Houthoofd, K.; Philippaerts, A.; De Jonghe, C.; Paul, J. S.; Jacobs, P. A.; Sels, B. F. *Green Chem.* **2010**, *12*, 1083−1089.
(20) Li, L.; Stroobants, C.; Lin, K.; Jacobs, P. A.; Sels, B. F.; Pescarmona, P. P. *Green Chem.* **2011**, *13*, 1175−1181.
(21) Román-Leshkov, Y.; Davis, M. E. *ACS Catal.* **2011**, *1*, 1566−1580.
(22) (a) Kimura, H. *Appl. Catal. A-Gen* **1993**, *105*, 147−158. (b) Garcia, R.; Besson, M.; Gallezot, P. *Appl. Catal. A-Gen* **1995**, *127*, 165−176. (c) Pagliaro, M.; Ciriminna, R.; Kimura, H.; Rossi, M.; Della Pina, C. *Angew. Chem., Int. Ed.* **2007**, *46*, 4434−4440. (d) Wörz, N.; Brandner, A.; Claus, P. *J. Phys. Chem. C* **2010**, *114*, 1164−1172.
(23) Dostalek, R.; Knuth, B.; Schneider, R. DE 19543415 A1, May 23, 1996.
(24) (a) ten Dam, J.; Kapteijn, F.; Djanashvili, K.; Hanefeld, U. *Catal. Commun.* **2011**, *13*, 1−5. (b) Auneau, F.; Michel, C.; Delbecq, F.; Pinel, C.; Sautet, P. *Chem.-Eur. J.* **2011**, *17*, 14288−14299.
(25) (a) Holm, M. S.; Saravanamurugan, S.; Taarning, E. *Science* **2010**, *328*, 602−605. (b) Holm, M. S.; Pagán-Torres, Y. J.; Saravanamurugan, S.; Riisager, A.; Dumesic, J. A.; Taarning, E. *Green Chem.* **2012**, *14*, 702−706.
(26) Assary, R. S.; Curtiss, L. A. *J. Phys. Chem. A* **2011**, *115*, 8754−8760.
(27) (a) Van de Vyver, S.; Geboers, J.; Dusselier, M.; Schepers, H.; Vosch, T.; Zhang, L.; Van Tendeloo, G.; Jacobs, P. A.; Sels, B. F. *ChemSusChem* **2010**, *3*, 698−701. (b) Geboers, J.; Van de Vyver, S.; Carpentier, K.; Jacobs, P. A.; Sels, B. *Chem. Commun.* **2011**, *47*, 5590−5592. (c) Shiju, N. R.; Alberts, A. H.; Khalid, S.; Brown, D. R.; Rothenberg, G. *Angew. Chem., Int. Ed.* **2011**, *123*, 9789−9793. (d) Stein, A.; Melde, B. J.; Schroden, R. C. *Adv. Mater.* **2000**, *12*, 1403−1419. (e) Van de Vyver, S.; Geboers, J.; Schutyser, W.; Dusselier, M.; Eloy, P.; Dornez, E.; Seo, J. W.; Courtin, C. M.; Gaigneaux, E. M.; Jacobs, P. A.; Sels, B. F. *ChemSusChem* **2012**, DOI: 10.1002/cssc.201100782.
(28) (a) Shylesh, S.; Wagener, A.; Seifert, A.; Ernst, S.; Thiel, W. R. *Angew. Chem., Int. Ed.* **2010**, *49*, 184−187. (b) Hoffmann, F.; Cornelius, M.; Morell, J.; Fröba, M. *Angew. Chem., Int. Ed.* **2006**, *45*, 3216−3251. (c) Wan, Y.; Wang, H.; Zhao, Q.; Klingstedt, M.; Terasaki, O.; Zhao, D. *J. Am. Chem. Soc.* **2009**, *131*, 4541−4550.
(29) (a) de Clippel, F.; Harkiolakis, A.; Ke, X.; Vosch, T.; Van Tendeloo, G.; Baron, G. V.; Jacobs, P. A.; Denayer, J. F. M.; Sels, B. F. *Chem. Commun.* **2010**, *46*, 928−931. (b) de Clippel, F.; Harkiolakis, A.; Vosch, T.; Ke, X.; Giebeler, L.; Oswald, S.; Houthoofd, K.; Jammaer, J.; Van Tendeloo, G.; Martens, J. A.; Jacobs, P. A.; Baron, G. V.; Sels, B. F.; Denayer, J. F. M. *Microporous Mesoporous Mater.* **2011**, *144*, 120−133.
(30) (a) Jun, S.; Joo, S. H.; Ryoo, R.; Kruk, M.; Jaroniec, M.; Liu, Z.; Ohsuna, T.; Terasaki, O. *J. Am. Chem. Soc.* **2000**, *122*, 10712−10713. (b) Joo, S. H.; Choi, S. J.; Oh, I.; Kwak, J.; Liu, Z.; Terasaki, O.; Ryoo, R. *Nature* **2001**, *412*, 169−172. (c) Lu, A.-H.; Schüth, F. *Adv. Mater.* **2006**, *18*, 1793−1805. (d) Liang, C.; Li, Z.; Dai, S. *Angew. Chem., Int. Ed.* **2008**, *47*, 3696−3717.
(31) Glover, T. G.; Dunne, K. I.; Davis, R. J.; LeVan, M. D. *Microporous Mesoporous Mater.* **2008**, *111*, 1−11.
(32) (a) Nakajima, K.; Okamura, M.; Kondo, J. N.; Domen, K.; Tatsumi, T.; Hayashi, S.; Hara, M. *Chem. Mater.* **2009**, *21*, 186−193. (b) Van de Vyver, S.; Peng, L.; Geboers, J.; Schepers, H.; de Clippel, F.; Gommes, C. J.; Goderis, B.; Jacobs, P. A.; Sels, B. F. *Green Chem.* **2010**, *12*, 1560−1563.
(33) (a) Stöber, W.; Fink, A.; Bohn, E. *J. Colloid Interface Sci.* **1968**, *26*, 62−69. (b) Grün, M.; Lauer, K. K.; Unger, I. *Adv. Mater.* **1997**, *9*, 254−257.
(34) (a) Teraoka, Y.; Ishida, S.; Yamasaki, A.; Tomonaga, N.; Yasutake, A.; Izumi, J.; Moriguchi, I.; Kagawa, S. *Microporous Mesoporous Mater.* **2001**, *48*, 151−158. (b) Casagrande, M.; Moretti, E.; Storaro, L.; Lenarda, M.; Gersisch, J.; Stievano, L.; Wagner, F. E. *Microporous Mesoporous Mater.* **2006**, *91*, 261−267.
(35) *Software PHI Multipak, V 6.1 A*; Physical Electronics, Inc., Eden Prairie: 1994−1999.
(36) Wang, J.; McEnaney, B. *Thermochim. Acta* **1991**, *190*, 143−153.
(37) Holm, T. *J. Chromatogr., A* **1999**, *842*, 221−227.
(38) Corma, A.; Iborra, S.; Mifsud, M.; Renz, M. *Arkivoc* **2005**, *9*, 124−132.
(39) (a) Wang, X.; Xu, H.; Fu, X.; Liu, P.; Lefebvre, F.; Basset, J. M. *J. Mol. Catal. A: Chem.* **2005**, *238*, 185−191. (b) Bhambhani, M. R.; Cutting, P. A.; Sing, K. S. W.; Turk, D. H. *J. Colloid Interface Sci.* **1972**, *38*, 109. (c) Mal, N. K.; Ramaswamy, A. V. *J. Mol. Catal. A: Chem.* **1996**, *105*, 149−158. (d) Shah, P.; Ramaswamy, A. V.; Lazar, K.; Ramaswamy, V. *Appl. Catal. A-Gen* **2004**, *273*, 239−248.
(40) (a) Romàn-Leshkov, Y.; Moliner, M.; Labinger, J. A.; Davis, M. E. *Angew. Chem., Int. Ed.* **2010**, *49*, 8954−8957. (b) Moliner, M.; Román-Leshkov, Y.; Davis, M. E. *Proc. Natl. Acad. Sci. U.S.A.* **2010**, *107*, 6164−6168.
(41) (a) Corma, A.; Nemeth, L. T.; Renz, M.; Valencia, S. *Nature* **2001**, *412*, 423−425. (b) Corma, A.; Domine, M. E.; Valencia, S. *J. Catal.* **2003**, *215*, 294−304. (c) Corma, A.; Navarro, M. T.; Renz, M. *J. Catal.* **2003**, *219*, 242−246. (d) Corma, A.; Renz, M. *Chem. Commun.* **2004**, 550−551. (e) Abdel-Fattah, T. M.; Pinnavaia, T. J. *Chem. Commun.* **1996**, 665−666.
(42) Corma, A.; Domine, M. E.; Nemeth, L.; Valencia, S. *J. Am. Chem. Soc.* **2002**, *124*, 3194−3195.
(43) (a) Chakraborty, B.; Viswanathan, B. *Catal. Today* **1999**, *49*, 253−260. (b) Busch, O. M.; Brijoux, W.; Thomson, S.; Schüth, F. *J. Catal.* **2004**, *222*, 174−179.
(44) Burket, C. L.; Rajagopalan, R.; Marencic, A. P.; Dronvajjala, K.; Foley, H. C. *Carbon* **2006**, *44*, 2957−2963.
(45) Boehm, H. P. *Carbon* **1994**, *32*, 759−769.
(46) (a) Otake, Y.; Jenkins, R. G. *Carbon* **1993**, *31*, 109−121. (b) Peric-Grujic, A. A.; Neskovic, O. M.; Veljkovic, M. V.; Lausevic, M. D.; Lausevic, Z. V. *J. Serb. Chem. Soc.* **2002**, *67*, 761−768. (c) Corthals, S.; Van Noyen, J.; Geboers, J.; Vosch, T.; Liang, D. D.; Ke, X. X.; Hofkens, J.; Van Tendeloo, G.; Jacobs, P.; Sels, B. *Carbon* **2012**, *50*, 372−384.
(47) (a) Vinke, P.; Van Der Elik, M.; Verbree, M.; Voskamp, A. F. *Carbon* **1994**, *32*, 675−686. (b) Rios, R. R.; Alves, D. E.; Dalmázio, I.; Bento, S. F.; Donnici, C. L.; Lago, R. M. *Mater. Res.* **2003**, *6*, 129−135.
(48) Gorgulho, H. F.; Mesquita, J. P.; Gonçalves, F.; Pereira, M. F. R.; Figueiredo, J. L. *Carbon* **2008**, *46*, 1544−1555.
(49) (a) Chen, S. G.; Yang, R. T.; Kapteijn, F.; Moulijn, J. A. *Ind. Eng. Chem. Res.* **1993**, *32*, 2835−2840. (b) Pérez-Mendoza, M.; Domingo-García, M.; López-Garzón, F. J. *Appl. Catal. A-Gen* **2002**, *224*, 239−253.
(50) Strelko, V., Jr.; Malik, D. J.; Streat, M. *Carbon* **2002**, *40*, 95−104.

(51) (a) de la Puente, G.; Pis, J. J.; Menendez, J. A.; Grange, P. *J. Anal. Appl. Pyrolysis* **1997**, *43*, 125−138. (b) Figueiredo, J. L.; Pereira, M. F. R.; Freitas, M. M. A.; Orfao, J. J. M. *Carbon* **1999**, *37*, 1379−1389.
(52) (a) Yumitori, S. *J. Mater. Sci.* **2000**, *35*, 139−146. (b) Lázló, K.; Josepovits, K.; Tombácz, E. *Anal. Sci.* **2001**, *17*, i1741−i1744.
(53) Nakajima, K.; Okamura, M.; Kondo, J. N.; Domen, K.; Tatsumi, T.; Hayashi, S.; Hara, M. *Chem. Mater.* **2009**, *21*, 186−193.
(54) (a) Zheng, A.; Zhang, H.; Lu, X.; Liu, S.-B.; Deng, F. *J. Phys. Chem. B* **2008**, *112*, 4496−4505. (b) Melero, J. A.; Stucky, G. D.; van Grieken, R.; Morales, G. *J. Mater. Chem.* **2002**, *12*, 1664−1670. (c) Morales, G.; Paniagua, M.; Melero, J. A.; Vicente, G.; Ochoa, C. *Ind. Eng. Chem. Res.* **2011**, *50*, 5898−5906.
(55) Rakiewicz, E.; Peters, A. W.; Wormsbecher, R. F.; Sutovich, K. J.; Mueller, K. T. *J. Phys. Chem. B* **1998**, *102*, 2890−2896.
(56) Wang, B.; Lee, C. W.; Cai, T.-X.; Park, S.-E. *Catal. Lett.* **2001**, *76*, 219−224.
(57) Peng, L.; Philippaerts, A.; Ke, X.; Van Noyen, J.; de Clippel, F.; Van Tendeloo, G.; Jacobs, P. A.; Sels, B. F. *Catal. Today* **2010**, *150*, 140−146.
(58) Hurtta, M.; Pitkänen, I.; Knuutinen, J. *Carbohydr. Res.* **2004**, *339*, 2267−2273.
(59) Assary, R. S.; Curtiss, L. A. *Energy Fuels* **2012**, *26*, 1344−1352.
(60) Serrano-Ruiz, J. C.; Braden, D. J.; West, R. M.; Dumesic, J. A. *Appl. Catal. B-Environ.* **2010**, *100*, 184−189.
(61) Saravanamurugan, S.; Riisager, A. *Catal. Commun.* **2012**, *17*, 71−75.
(62) Lourvanij, K.; Rorrer, G. L. *J. Chem. Technol. Biotechnol.* **1997**, *69*, 35−44.
(63) (a) Hegner, J.; Pereira, K. C.; DeBoef, B.; Lucht, B. L. *Tetrahedron Lett.* **2010**, *51*, 2356−2358. (b) Vandam, V. E.; Kieboom, A. P. G.; Vanbekkum, H. *Starch/Staerke* **1986**, *38*, 95−101. (c) Mehdi, H.; Fabos, V.; Tuba, R.; Bodor, A.; Mika, L. T.; Horvath, I. T. *Top. Catal.* **2008**, *48*, 49−54.
(64) Van de Vyver, S.; Thomas, J.; Geboers, J.; Keyzer, S.; Smet, M.; Dehaen, W.; Jacobs, P. A.; Sels, B. F. *Energy Environ. Sci.* **2011**, *4*, 3601−3610.